

INSTITUTO TECNOLÓGICO Y DE ESTUDIOS
SUPERIORES DE MONTERREY



MASTERS THESIS PROPOSAL

**Fabrication of graphitic-carbon suspended
nanowires through
mechanoelectrospinning of
photocrosslinkable polymers**

Author:

**Antonio Osamu KATAGIRI
Tanaka**

Principal Advisor:

**Dr. Héctor Alán AGUIRRE
Soto**

Co-advisor and

Director of Program:

**Dra. Dora Iliana MEDINA
Medina**

*A thesis proposal submitted in fulfillment of the requirements
for the degree of Master of Science in Nanotechnology (MNT)*

in

**ITESM Campus Estado de México
School of Engineering and Sciences**

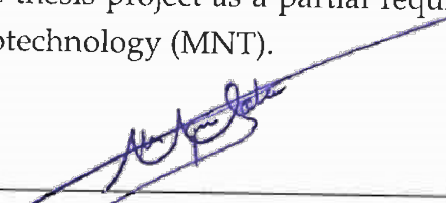
Estado de México, Atizapan de Zaragoza, May 16, 2019

INSTITUTO TECNOLÓGICO Y DE ESTUDIOS SUPERIORES DE
MONTERREY


Campus Estado de México

Supervising Committee

The committee members, hereby, recommend that the proposal by Antonio Osamu KATAGIRI Tanaka to be accepted to develop the thesis project as a partial requirement for the degree of Master of Science in Nanotechnology (MNT).



Dr. Héctor Alán AGUIRRE Soto
Tecnológico de Monterrey
Principal Advisor



Dra. Dora Iliana MEDINA Medina
Tecnológico de Monterrey
Co-Advisor

Dr. Marc MADOU
Tecnológico de Monterrey
Committee Member

Dr. Sergio Omar MARTÍNEZ Chapa
Tecnológico de Monterrey
Committee Member

Dra. Dora Iliana MEDINA Medina
Director of Program in Nanotechnology
School of Engineering and Sciences

Estado de México, Atizapan de Zaragoza, May 16, 2019

Contents

Supervising Committee	i
Abstract	vi
1 Introduction	1
2 Problem Definition and Motivation	3
3 Hypothesis and Research Questions	5
3.1 Research Hypothesis	5
3.2 Research Questions	5
4 Objectives	7
4.1 General objective	7
4.2 Specific objectives	7
5 Related Work	8
5.1 Role of rheological properties in near field electrospun fibers morphology [8]	8
5.1.1 Rheometry	8
Amplitude Sweep	8
Frequency Sweep	9
Flow Curve	9
5.1.2 Sample Preparation	10
5.1.3 Rheological Characterization : Amplitude Sweep	11
5.1.4 Rheological Characterization : Flow Curve	12
5.1.5 Rheological Characterization : Frequency Sweep	14
5.2 Advanced Manufacturing Techniques for the Fabrication and Surface Modification of Carbon Nanowires [6]	18
5.2.1 Method 1 :	19
SU-8 2002 Polymer Solution	19
Deposition of Electrospun SU-8 2002 Solution	19
5.2.2 Method 2 :	20
SU-8 2025 Polymer Solution	20
Deposition of Electrospun SU-8 2025 Solution	20
5.2.3 Results and Discussion	20

6	Theoretical Framework	21
6.1	Photoresists	21
6.2	Electro-Mechanical Spinning	22
6.3	Pyrolysis	24
6.4	Carbon nano-wire	25
6.5	Polymer Solutions	26
6.6	Preliminary Experiments	26
6.6.1	Materials and Sample Preparation	26
6.6.2	Results	28
7	Methodology	31
7.1	Preliminary Literature Review	31
7.2	Evaluation of Fabrication Parameters	31
7.3	Polymer Solution Design	32
7.4	Fabrication of Carbon Nano-wires	32
7.5	Data Collection and Analysis of Results	33
7.6	Documentation	33
8	Work Plan	34

List of Figures

1.1	Fabrication Process	1
5.1	Amplitude Sweep	9
5.2	Frequency Sweep	9
5.3	Flow Curves	10
5.4	Serie A - Amplitude Sweep	11
5.5	Serie B - Amplitude Sweep	12
5.6	Serie C - Amplitude Sweep	13
5.7	Serie A - Flow curve	13
5.8	Serie B - Flow curve	14
5.9	Serie C - Flow curve	14
5.10	Serie A - Frequency Sweep	15
5.11	Serie B - Frequency Sweep	16
5.12	Serie C - Frequency Sweep	16
6.1	Positive and negative resist exposure and development	22
6.2	Far Field Electrospinning set-up	24
6.3	Near Field Electrospinning set-up	25
6.4	Effects in polymer chains dimensions due to solvent quality	26
6.5	Effects of electrolyte in polymer chain dimensions	26
6.6	Set 1 of the Recreation of Flores' "Serie B" Samples	27
6.7	Set 2 of the Recreation of Flores' "Serie B" Samples	28
6.8	Set 1 Flow Curve Characterization of the Recreation of Flores' "Serie B" Samples	29
6.9	Set 2 Flow Curve Characterization of the Recreation of Flores' "Serie B" Samples	29

List of Abbreviations

CEM	Campus Estado de México
CNWs	Carbon Nano-wires
DC	Direct Current
EMS	Electromechanical Spinning
FFES	Far Field de Electrospinning
ITESM	Instituto Tecnológico y de Estudios Superiores de Monterrey
MA	Massachusetts
MEMS	Microelectromechanical Systems
MNT	Maestría en Nanotecnología (<i>Master of Science in Nanotechnology</i>)
MTY	Monterrey <i>or</i> Campus Monterrey
NFES	Near Field de Electrospinning
USA	United States of America
UV	Ultraviolet

INSTITUTO TECNOLÓGICO Y DE ESTUDIOS SUPERIORES DE
MONTERREY

Abstract

Faculty: Nanotechnology

School of Engineering and Sciences

Master of Science in Nanotechnology (MNT)

**Fabrication of graphitic-carbon suspended nanowires through
mechanoelectrospinning of photocrosslinkable polymers**

by Antonio Osamu KATAGIRI Tanaka

Carbon nano-wires are versatile materials composed of carbon chains with a wide range of applications due to their high conductivity. Regardless of the high interest in the implementation of carbon nano-wires in several applications and devices, no feasible processes have been developed to fabricate carbon nano-wires with spatial control at a reasonable cost. Carbon nano-wires have been fabricated with the use of a photoresist, but little is known about polymers that can produce more conductive carbon nano-wires after pyrolysis. Various polymer solutions have been tested in near field electrospinning (NFES) and photopolymerization separately, however, few have been tested for nano-wire fabrication purposes through pyrolysis. The intention behind the thesis proposal is to implement rheology analyses of different polymer solutions to determine if they can be easily electrospun at low voltages and then fabricate nano-wires with them. This thesis work arises from the need to test a greater variety of polymers with the goal to design a polymer solution to fabricate carbon nano-wires with better conductivity than the current SU-8 polymeric nano-fibers. The research process will include the design of polymer solutions that can be electrospun, photopolymerized, and then pyrolyzed into conducting carbon nanowires. On the other hand, it is intended to engineer a newly designed polymer solution to achieve mass scale manufacturing of conductive carbon nano-wires in an inexpensive, continuous, simple and reproducible manner as central components for nano-sensors.

keywords: nanotechnology, carbon, nano-wires, electrospinning, NFES

1 Introduction

Carbon nano-materials are subjected to great interest for research purposes due to their various potential applications in diverse areas that take advantage of the nano-scale properties. [27] Carbon nano-materials are suitable for catalysis, adsorption, carbon capture, energy and hydrogen storage, drug delivery, bio-sensing, and cancer detection. [27] Some matchless properties that allow carbon nano-materials to be utilized within multiple functionalities include high porosity, distinguished structures, uniform morphologies, high stability, high magnetic properties, and high conductivity. [27]

This document bestows a thesis proposal to perform a research to engineer and design a polymer solution to achieve mass scale manufacturing of high conductive carbon nano-wires with a reduced diameter in an inexpensive, continuous, simple and reproducible manner. The research intends to involve several manufacturing processes such as near field electrospinning, photopolymerization, pyrolyzation, and carbonization, as they have shown to be promising methods for the fabrication of carbon nano-materials. [6] See Figure 1.1. A number of processes have been developed for specific purposes of polymeric nano-fibers, some include surface deposition, composites, and chemical adjustments. Polymeric nano-fibers must be also pyrolyzed to generate carbon nano-wires with conductive capabilities [16] for electrochemical sensing and energy storage purposes.

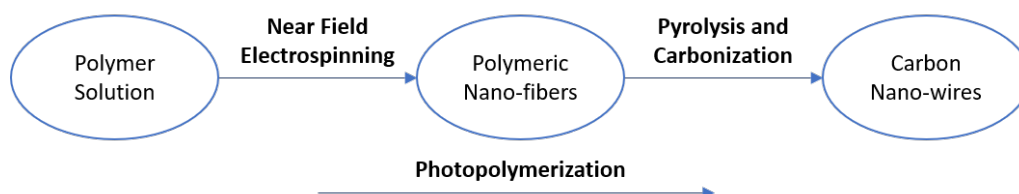


FIGURE 1.1: Fabrication process of conductive carbon nano-wires to achieve through the proposed dissertation.

Nanotechnology has led to the study of different polymer patterning techniques to integrate carbon nano-wires structures. One technique is known as far-field electrospinning, a process in which electrified jets of polymer solution are dispensed to synthesize nano-fibers which are then pyrolyzed at high temperatures. One sub-technique derived from electrospinning is near field electromechanical spinning or EMS. EMS has proved to deliver high control in patterning polymeric nano-fibers. [6]

The proposal is to continue the previous work done in regards to the synthesis of carbon nano-wires. Previous work includes the fabrication of suspended carbon nano-wires by two methods: electro-mechanical spinning and multiple-photon polymerization with a photoresist. [6] This research proposal is intended to focus on electro-mechanical spinning processes only, to bring off polymer solutions that can be electrospun by near field electrospinning (NFES), photopolymerized and pyrolyzed into conducting carbon nano-wires. The polymer solutions described by Cardenas [6] are to be amended to achieve the goal mentioned in the previous statement.

Traditional near-field electrospinning or NFES allows large scale manufacturability combined with spatial control of material deposition. [16] However, the reported efforts required the use of electric fields in excess of 200 kV/m for continuous operation, resulting in limited control for nano-fiber patterning in traditional NFES processes. Madou et al. [16] conclude that the current state-of-the-art synthesis processes for polymer nano-fibers lack to yield precise, inexpensive, fast, and continuous manufacturing properties.

2 Problem Definition and Motivation

Carbon nanowires have been fabricated with a photoresist by multiple-photon polymerization techniques. However little is known about polymers that can produce conductive carbon nano-wires after pyrolysis, as it is generally believed that most polymers do not form significant amounts of graphitic carbon when carbonized. In the past years, photopolymerization processes have been applied to the fabrication of nano-structures with the use of an epoxy based photoresist. [5] Photopolymerization techniques deliver patterning resolutions with nano-scale tolerances through two-photon lithography for the production of highly detailed structures [10].

On the other hand, electrospinning has been acknowledged as a process with promising results at nano-structure fabrication [5], yet there is little research regarding the implementation of electrospinning for the fabrication of carbon nano-wires. Electrospinning has the potential to be a more straightforward process for the design and fabrication of nano-structures, as it can achieve mass scale manufacturing in a continuous, simple and reproducible manner. Cardenas [6] showed that electrospinning can be implemented with ease for carbon nano-wire synthesis. Mechano-electrospinning, a new variant of electrospinning shows promising results in the production of ordered carbon nano-wires. As stated in [6], mechano-electrospinning is an early technology invention and brings new challenges, such as the reproducibility of carbon nano-wire production. Furthermore, the study of a new fabrication process to produce carbon nanowires that involves mechano-electrospinning will enable spatial control of the structures' patterning.

Since electrospinning seems to be a better alternative for carbon nano-wire

fabrication processes; and for that purpose of its implementation, it is required to develop polymer solutions that can be mechano-electrospun, photopolymerized and pyrolyzed into conducting carbon nano-wires. Carbon nano-materials have been subjected to research due to their various potential applications in diverse areas that take advantage of the nano-scale properties. [27] Carbon nano-materials are suitable for the catalysis, adsorption, carbon capture, energy and hydrogen storage, drug delivery, bio-sensing and cancer detection. [27] However most applications are not currently feasible due to the lack of a continuous, simple and reproducible fabrication method with inexpensive processes. With the newly designed polymer solution, it would be possible to produce carbon nano-wires in large quantities, and therefore more applications will become feasible. On the other hand, the new technique will overcome some limitations of other methods such as lithography currently has. For instance, patterns created by lithography processes cannot be originated, only replicated, all constituent points of the pattern can only be addressed at the same time, and the process requires the pattern to be encoded into a mask. [13]

3 Hypothesis and Research Questions

3.1 Research Hypothesis

The rheological properties of polymer solutions along with synthesis parameters (stage velocity, voltage, dispense rate) can be amended through rheological analyses to obtain a low voltage electrospun-able, photopolymerizable and graphitizable fibers for the fabrication conductive of carbon nano-wires with specified dimensions (diameter and length). The rheological properties of polymer solutions along with synthesis parameters are to be amended by replacing the PEO (Poly(ethylene) oxide) component within the existing polymer solutions described in Flores [8] and Cardenas [6] work. PEO is to be replaced as its only purpose is to allow the electrospinning process to take place, but no benefit is obtained from it after pyrolysis.

3.2 Research Questions

- Is there any evidence of conductive carbon nano-wire fabrication though electrospun-able and pyroizable polymer solutions?
- What are the process parameters to consider/control for the fabrication processes of carbon nano-wires?
- What rheological properties are to be controlled/tested to deliver an electrospun-able and pyroizable polymer solution?
- Are there any efforts employed to the design of polymer solutions that can be electrospun, photopolymerized, and pyrolyzed into conducting carbon nanowires?

- What are the optimal fabrication parameters for the synthesis of carbon nano-wires through near-field electromechanical spinning?
- What materials can be used to ease the electrospinning process and favor the carbon nano-wire properties after pyrolysis?

4 Objectives

4.1 General objective

Study the practice and feasibility of a new fabrication process to achieve mass scale manufacturing of carbon nano-wires in an inexpensive, continuous, simple and reproducible manner; by the integration of mechano-electrospinning technique.

4.2 Specific objectives

- Design polymer solutions that can be electrospun by NFES, photopolymerized, and then pyrolyzed.
- Through rheological analyses, determine if polymer solutions can be easily employed for conducting carbon nano-wire synthesis.
- Determine and control the polymer solution rheological properties along with the process parameters of carbon nano-wire synthesis.
- Discover a PEO-similar material to allow the electrospinning process as well as input favourable properties to the carbon nano-wire yield.

5 Related Work

The following is a literature review to highlight the work done by others that is related to the proposed dissertation. This section presents the work that the proposal is based on to show others attempts to solve a problem related to Section 2.

5.1 Role of rheological properties in near field electrospun fibers morphology [8]

5.1.1 Rheometry

Rheometry is the measuring technology used to determine rheological data. There are different measuring systems, instruments and analysis methods. Both, liquids and solid can be investigated using rotational and oscillatory rheometers. Rotational tests are performed to characterize viscous behavior. In order to evaluate viscoelastic behavior, creep tests, relaxation tests and oscillatory tests are performed [8].

Amplitude Sweep

An amplitude sweep is a typical test used to characterize the behavior of a polymer solution or polymer melt. In this basic test a constant angular frequency is applied along with an increasing or decreasing deformation or strain, see Figure 5.1 a). The obtained results are the storage and loss moduli, G' and G'' respectively, along the values of percentage of strain applied. The amplitude is the maximum of the oscillatory motion. Normally at low frequencies the viscoelastic material presents a linear behavior, this is when the viscoelastic properties are independent of the strain or stress imposed due to the structure of the material stays undisturbed. Nevertheless, as the amplitude is increased at some at some point this linear trend changes suddenly. Once this critical amplitude value is reached the material becomes more elastic or viscous depending on the solution initial state, see Figure 5.1 b) [8].

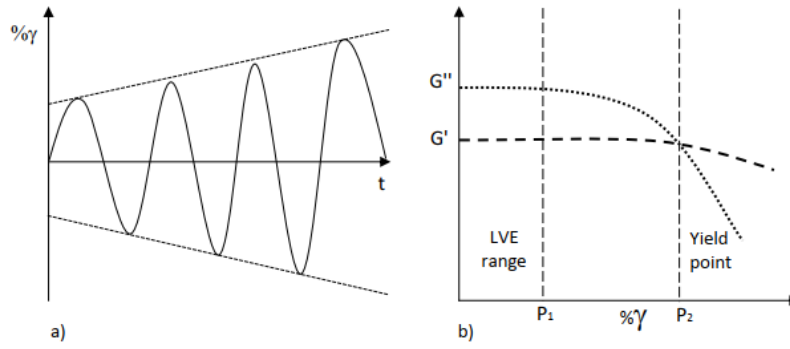


FIGURE 5.1: a) Imposed amplitude along time with constant frequency. b) Results for an amplitude sweep [8]

Frequency Sweep

A frequency sweep, is a common oscillatory test useful to understand the rheological behavior of fluids as it measures the viscoelastic properties. This measurement is considered a viscoelastic spectrum, in general, the shorter the timescale the more elastic the material behaves. These results are related to the molecular structure of the sample. Figure 5.2 shows a typical data for a polymer melt where different regions are observed. Frequency sweep measurements also allow the estimation of the molecular weight distribution characteristics such as entanglement density and process-ability [8].

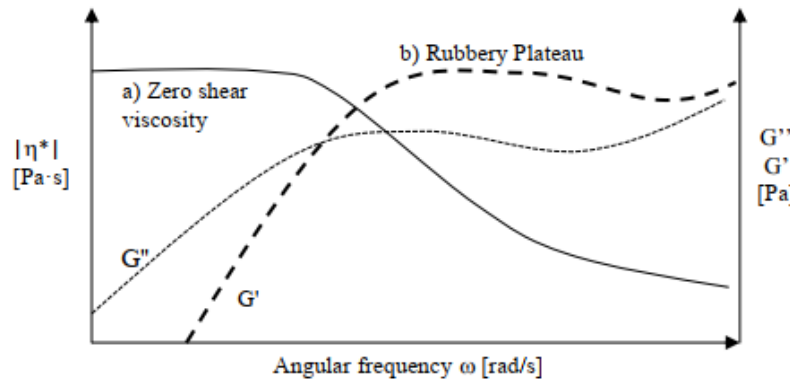


FIGURE 5.2: Typical results for a frequency sweep. [8]

Flow Curve

The viscosity is measured as a function of the shear rate in a rotational rheometer with different geometries according to the sample. Normally three types of behaviours can be characterized in flow curve measurements: a) ideal viscous, b) shear thinning and c) shear thickening. Figure 5.3 shows three different materials and their response to an imposed shear rate [8].

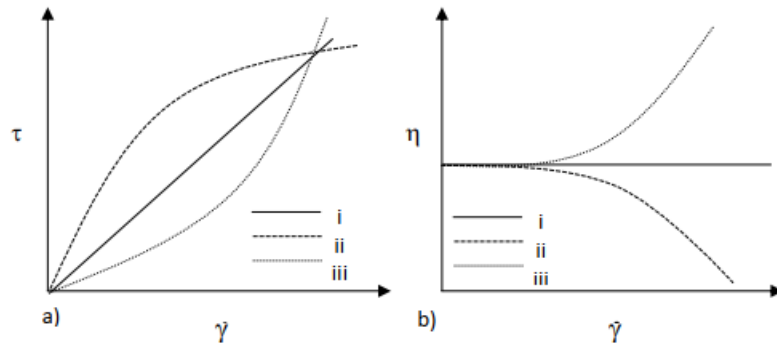


FIGURE 5.3: a) Flow curve stress vs stress. b) Flow curve strain vs shear viscosity. Both figures for i Newtonian fluid, ii Shear thinning fluid, iii Shear thickening fluid. [8]

5.1.2 Sample Preparation

Flores studied SU-8 2002 polymer solutions in cyclopentanone with poly(ethylene) oxide (PEO) and tetrabutylammonium tetrafluoroborate (TBATFB). For that purpose, several samples were prepared with the adequate amounts of PEO and TBATFB with 5 *ml* of SU-8 2002 and stirred at 160 *rpm* for one hour at 75 °C in the absence of light. A 5 *ml* syringe was used to extract the solution from the preparation vial. Finally the syringe was placed upside down for 24 hours to get rid of any bubbles within the solution. Table 5.1 lists the set of samples that were prepared as values in *wt%*, dissolved in SU-8 2002.

TABLE 5.1: Set of prepared samples [8]

	Serie A		Serie B		Serie C	
Sample	PEO	TBATFB	PEO	TBATFB	PEO	TBATFB
1	0.00	0.00	0.00	0.50	0.50	0.00
2	0.25	0.25	0.25	0.50	0.50	0.25
3	0.50	0.50	0.50	0.50	0.50	0.50
4	0.75	0.75	0.75	0.50	0.50	0.75
5	1.00	1.00	1.00	0.50	0.50	1.00

All the samples were executed in a rheometer (Physica MCR 301, Anton Paar) with a cone-and-plane geometry of diameter 24.979 *mm*, angle 4.014° and truncation of 249 μm . The measurements were performed at a temperature of 25 ± 0.1 °C. For amplitude sweep measurements, the angular frequency was settled at 10 s^{-1} , and the percentage amplitude gamma $\% \gamma$, was varied from 0.1 to 1000%. In flow curve tests, shear rate was applied from 0.1 to 100 s^{-1} . For frequency sweeps, the percentage of amplitude gamma, $\% \gamma$, was varied from 0.1 to 100 s^{-1} . During the measurements, the rheometer sample

area was saturated with cyclopentanone to avoid solvent evaporation.

5.1.3 Rheological Characterization : Amplitude Sweep

The "Serie A" result measurements indicate that the storage modulus G' is smaller than the loss modulus G'' . Both moduli have a parabolic behaviour. At low deformation the values of the moduli increase until they become stable at between 1 and 10 % γ . After the stabilization, both modulus start to decrease. The increase of PEO and TBATFB concentration G' and G'' also increase. Figure 5.4 shows the amplitude sweep for the samples of "Serie A".

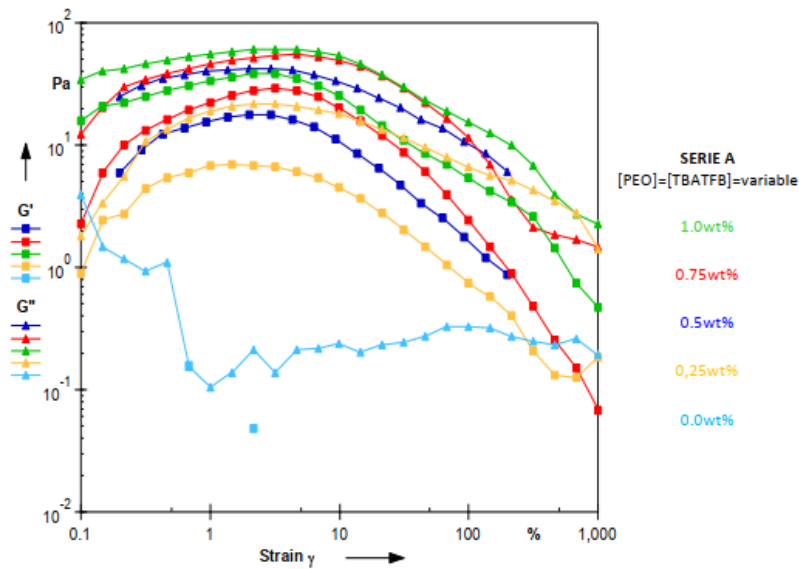


FIGURE 5.4: Serie A - Amplitude Sweep [8]

The results within Figure 5.4 showed that no clear linear viscoelastic region is present. The material has influenced by small deformations, hence it is very sensitive to external forces. No yield point was encountered as the moduli separate from each other with the increase of deformation.

Figure 5.5 illustrates the results obtained from the amplitude sweeps of Serie B samples. As shown in the figure, the concentration of 0 wt% shows a constant viscous modulus at 0.2 Pa. the 0.25 wt% concentration sample presented a similar behaviour to the 0 wt% sample but with a constant value of G' at 2 Pa. The other concentrations show a similar parabolic behaviour as the ones in Serie A.

The amplitude sweep results of Serie C are depicted in Figure 5.6. Similar to series A and B, results show that the storage modulus G' is smaller than the

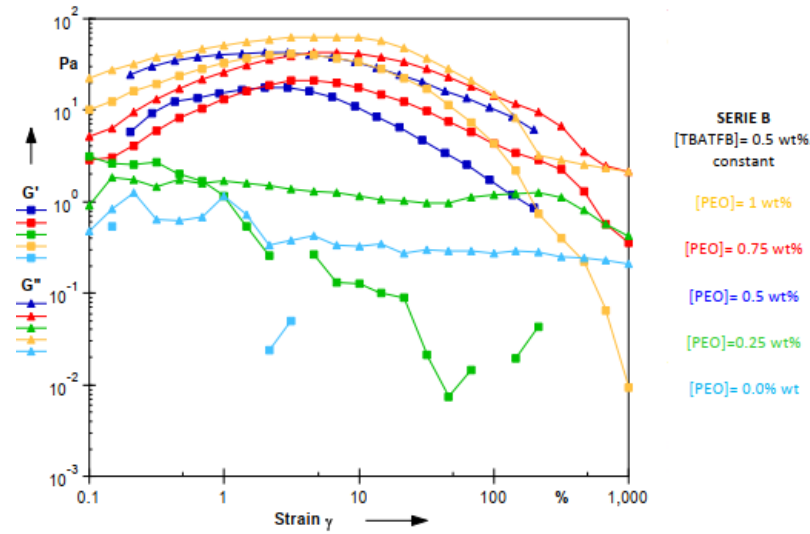


FIGURE 5.5: Serie B - Amplitude Sweep [8]

loss modulus G'' with a parabolic behaviour. Typically, the amplitude sweep is to determine the amplitude to be used in frequency sweeps. The amplitude determined by the amplitude sweeps shall keep the material structure undisturbed is known as the linear viscoelastic region (LVER). However, no LVER was found in the samples. For that reason, the percentage of amplitude gamma $\% \gamma$ was found by trial and error. Flores discovered that a $\% \gamma = 20$ has the best performance.

5.1.4 Rheological Characterization : Flow Curve

Figure 5.7 shows evidence that the equal increase of PEO and TBATFB concentrations result in an increase of shear viscosity rate $\dot{\gamma}$. For concentrations from 1.00 to 0.25 wt%, a slight increase of flow curve strain η for low shear rates to 0.3 s^{-1} . For shear rates greater than 0.3 s^{-1} , the η starts to decrease, as the polymer entanglements start to break apart, reducing friction between the polymer threads and therefore the viscosity also is reduced. The solution samples show a Newtonian-like behaviour and that may be caused by the use of the solvent cyclopentanone and by the small sized SU-8 2002 molecules.

From the results in Figure 5.7, it is noticeable that the addition of small amounts of PEO and TBATFB cause a change of one order of magnitude in shear viscosity in small concentrations and a triple change in high concentrations.

Series B flow curve results (Figure 5.8) do not show a clear correlation between PEO concentrations and shear viscosity. For PEO of 1 wt%, a slow

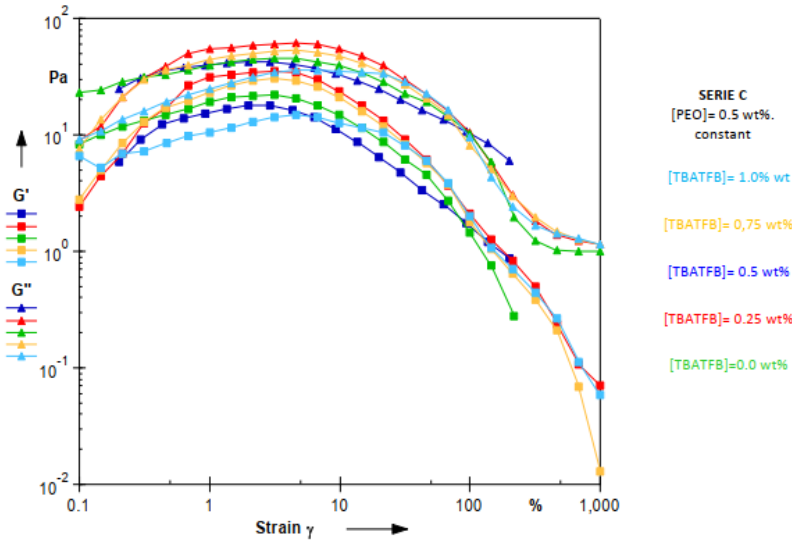


FIGURE 5.6: Serie C - Amplitude Sweep [8]

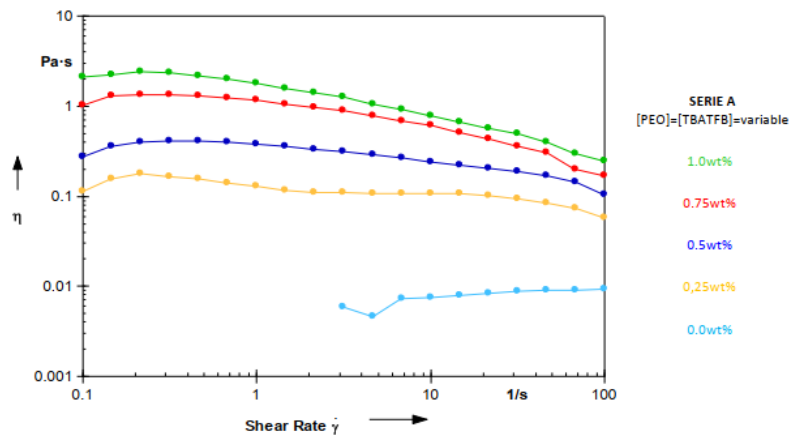


FIGURE 5.7: Serie A - Flow curve [8]

increase in η is present with the increase of shear rate, after γ drops from 2 to 0.8 $\text{Pa}\cdot\text{s}$, a shear thinning behaviour is present. For 0.50 and 0.75 $\text{wt}\%$ concentrations, a shear thinning behaviour is present throughout the plot. For the 0.50 $\text{wt}\%$ sample, viscosity value varied between 0.2 and 0.4 $\text{Pa}\cdot\text{s}$; and between 0.5 and 2.0 $\text{Pa}\cdot\text{s}$ for the 0.75 $\text{wt}\%$ sample. Viscosity is stabilized at 0.1 $\text{Pa}\cdot\text{s}$ when the shear rate is between 1 and 20 $\%$ for the sample of PEO $\text{wt}\%$. After stabilization, the viscosity decreases from 0.1 to 0.02 $\text{Pa}\cdot\text{s}$ for shear rates between 20 to 100 s^{-1} . For PEO 0.00 $\text{wt}\%$, a high variation is present in viscosity readings due to the presence of electrolytes cause amendments in the polymer chain within the solution.

The flow curve results of Serie C are presented in Figure 5.9. The sample with

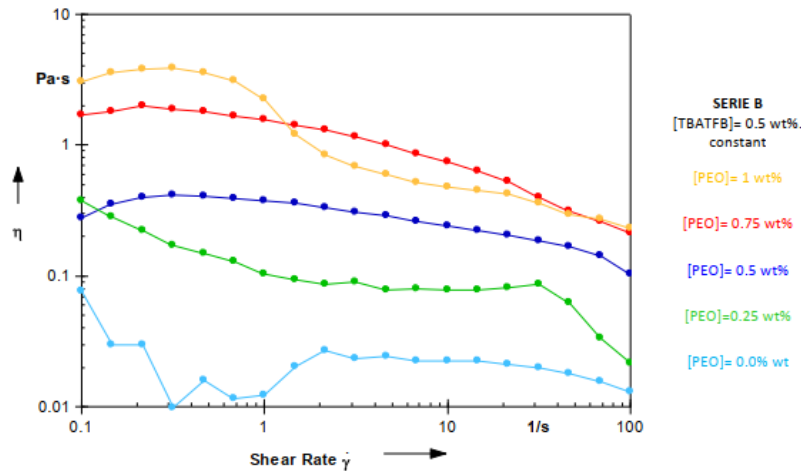


FIGURE 5.8: Serie B - Flow curve [8]

1 *wt%* TBATFB concentration shows a shear thinning behaviour for shear rates varying between 0.1 to 15 s^{-1} . The 1 *wt%* sample describes a drop in viscosity for shear rates between 15 to 20 s^{-1} followed by a stable state. A similar behaviour is observed for a concentration of 0.75 *wt%*, and less evident for 0.0 *wt%*. For concentrations of 0.5 *wt%* and 0.25 *wt%* the behaviour of the shear viscosity is similar.

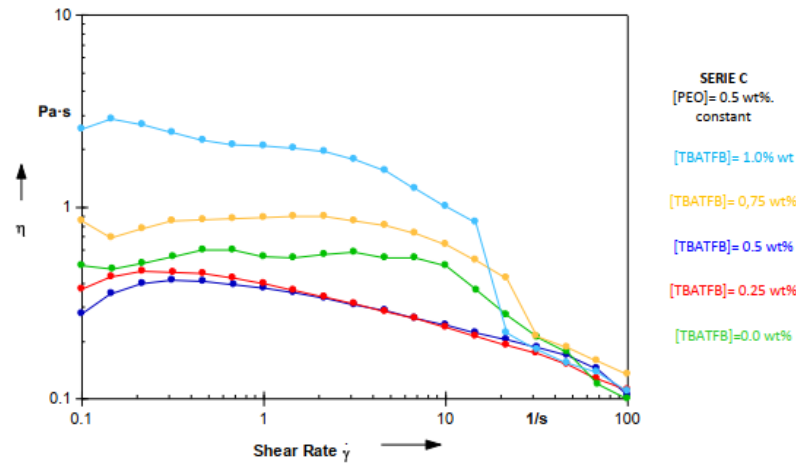


FIGURE 5.9: Serie C - Flow curve [8]

5.1.5 Rheological Characterization : Frequency Sweep

Figure 5.10 shows that the solution with the lowest concentration of PEO and TBATFB has a decreasing behaviour of the viscosity, but for values greater to 3 s^{-1} in frequency, the viscosity starts to increase. The solutions from 0.25 *wt%* to 1.00 *wt%* have the same shear-thinning behaviour. A direct relation between the concentrations and the viscosity values is discovered, where a

small drop of viscosity is presented with the decrease of additive concentration.

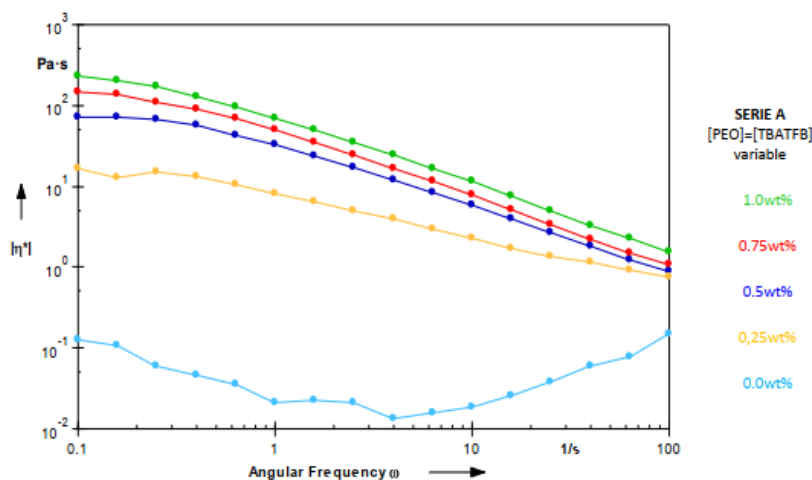


FIGURE 5.10: Serie A - Frequency Sweep [8]

Figure 5.11 shows the frequency sweep results from Serie B. The presented behaviour is similar to Serie A. for the lower concentrations of PEO, the equipment has not enough sensibility to make measurements of the storage modulus because this one is very low. At PEO 0.25 *wt%*, the viscosity remains almost constant at 1 *Pa.s*, but as in Serie A a little variation of viscosity is presented at the lowest values of angular frequency. On the other hand, for the 0.5, 0.75 and 1.00 *wt%* concentrations, the viscosity is similar. At 100 s^{-1} , the three high concentration samples converge to 2 *Pa.s*. It is imperative to assume that 0.5 *wt%* is the critical concentration, under this concentration the systems present different behaviours since the molecules have enough room to diffuse and break entanglements. When the critical entanglement concentration is exceeded, the polymer threads overlap and become tangled, therefore no more entanglements are no longer possible.

The frequency sweep behaviours of Serie C are presented in Figure 5.12. The figure does not indicate a clear correlation between the viscosity and the addition of TBATFB. All samples have a similar behaviour and magnitude, except for the 0.75 *wt%* TBATFB concentration sample as it presents a non uniform behaviour. At low frequencies, the viscosity increases, then it remains constant at 20 *Pa.s* until a frequency value of 4 s^{-1} ; the viscosity drastically decreases to 1 *Pa.s* and remains constant at that value. The 1.00 *wt%* sample has a decreasing viscosity behaviour at higher angular frequencies.

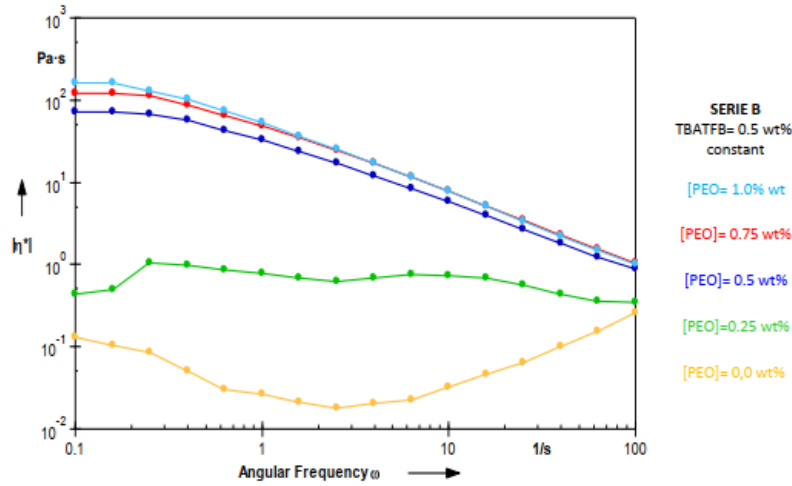


FIGURE 5.11: Serie B - Frequency Sweep [8]

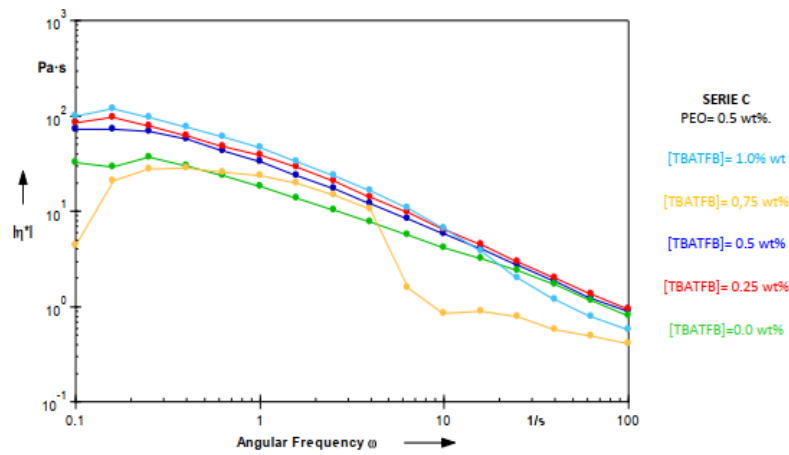


FIGURE 5.12: Serie C - Frequency Sweep [8]

Flores work [8] carried out a series of experiments in order to correlate the rheological properties of polymer solutions used in electro-mechanical spinning processes for the fabrication of carbon micro structures. Shear flow and dynamic measurements tests such as flow curves, amplitude sweeps and frequency sweeps were carried in an oscillatory rheometer to study the rheological behaviour of polymeric solutions of SU-8 2002, an epoxy-based negative photoresist, Poly(ethylene) oxide (PEO), a flexible, non-ionic polymer, and TBATFB (Tetrabutylammonium tetrafluoroborate) that acts as an electrolyte.

The concentrations of additives were varied from 0 *wt%* to 1.0 *wt%* with increments of 0.25. To observe the effects of each additive it was proposed a set of concentrations where both additives were equally varied (Serie A), TBATFB was constant the only PEO variations (Serie B), and PEO constant

concentration with TBATFB variations (Serie C). It was found that the variation of the additives (PEO and TBATFB) affects the rheological behavior of the solution. Typically, the addition of PEO increase the elongational and shear viscosities while the addition of TBATFB modifies this property but in a non-predictable manner. The solutions do not present yield stress as can be seen in Amplitude Sweep and Frequency Sweep measurements.

5.2 Advanced Manufacturing Techniques for the Fabrication and Surface Modification of Carbon Nanowires [6]

As stated by Cardenas [6], the following parameters play an important role in the graphitic content on the fabrication of carbon nano-wires through electrospinning:

1. The thickness of the produced polymeric wires,
2. the chemical composition and viscoelasticity of the polymeric solution,
3. the molecular alignment of the polymer,
4. the heat treatment temperature,
5. the mechanical pulling on the polymer jet during electrospinning,
6. the alignment of polymer chains induced by the presence of an electric field, and
7. the catalysts and solvents within the polymer solution.

Cardenas reviewed different polymer fabrication techniques and materials to produce carbon nano-wires. Within Cardenas' work the following parameters were evaluated to study the desirable characteristics for building highly sensitive sensor devices: a) the chemical composition and viscoelasticity of the polymer solution, b) the thickness of the produced polymeric wires, c) the mechanical pulling on the polymeric jet during electrospinning, and d) the alignment of the polymer chains induced by the presence of an electric field. Cardenas' work states that various methods are implemented to produce nanofibers, such as laser ablation, chemical vapor deposition, discharge, and vapor growth. However, those techniques are abandoned due to their low yield output and expensive equipment. Whereas electrospinning (ES) of polymer solutions is a promising technique for simple and inexpensive fabrication of carbon nano-wires, which can be combined with a moving collector to yield even thinner fibers.

The production of carbon structures involves to main procedures: a) polymer patterning such as photolithography, electrospinning, Computer Numerical

Control (CNC), molding, hot embossing, and recently, Multiple Photon Polymerization; and b) carbonization, which induces further thinning of the patterned polymer and its conversion into carbon. Cardenas conducted some experiments to characterize and analyze carbon nano-wires. Polymeric SU-8 nano fibers were produced by two different methods; for each method different polymer solutions were employed, See Table 5.2.

TABLE 5.2: Method 1 and Method 2 conditions and parameters [6]

Conditions and Parameters	Method 1	Method 2
Solution materials	SU-8 2002, PEO and TBATFB	SU-8 2025, TBATFB and SU-8 thinner
Solution preparation	stirred for 1 <i>hr</i> at 75°C at 100-150 <i>rpm</i>	stirred for 1.5 <i>hrs</i> at 75°C at 100 <i>rpm</i>
Deposition voltage	100 V	200 V (due to the higher viscosity)
Results	failed the pyrolyzation process	81% yield rate after pyrolyzation
Fiber diameter	NA	204 <i>nm</i>

5.2.1 Method 1 :

SU-8 2002 Polymer Solution

The polymeric solution was composed by 2 *ml* of SU-8 2002 mixed with 0.5 *wt%* of PEO and 0.5 *wt%* of TBATFB to increase its conductivity and yield soother polymer jets during electrospinning. Magnetic stirring was performed for 1 *hr* at 75 °C with *rpm* values between 100 and 150.

Deposition of Electrospun SU-8 2002 Solution

A voltage around 100 V was applied between a dispensing needle and the collector stage. The needle to collector distance was set to 100 μm . The collector was attached to a mechanically motorized stage, which allowed the SU-8 nanofibers patterning into the SU-8 microstructures. Three different stage velocities were tested (20,40 and 60 *mm/s*) to study the influence on the wire geometry. Acceleration of the stage was set to 500 *mm/s*². After deposition, samples were exposed to UV light for 45 *min* to complete cross-linking.

5.2.2 Method 2 :

SU-8 2025 Polymer Solution

The solution was composed of 4 *ml* of SU-8 2025, 4 *mg* of TBATFB and 80 μL of SU-8 thinner. The solution was stirred for 1.5 *hrs* at 100 *rpm* at 75 °C.

Deposition of Electrospun SU-8 2025 Solution

To pattern the fiber exactly on top of the SU-8 electrodes, a routine was set to move the needle relative to the collector. The polymer solution was dispensed at a rate of 8.847 *nL/min* using a programmable syringe pump. A voltage of 200 *V* was applied between the collector plate and the needle tip, and the polymer solution was allowed to flow for between 15 to 30 *min* until it was stable. A higher voltage had to be applied compared to Method 1 due to the higher viscosity of the SU-8 2025 solution. Once a steady flow was achieved, the collector was moved relative to the needle tip using the motorized stage. The mechanical parameters used during were: a) velocity of 5000 $\mu\text{m/s}$, an acceleration of 2500 $\mu\text{m/s}^2$. The sample was exposed to UV light for 45 *min* to ensure complete cross-linking of the deposited SU-8 nanofiber.

5.2.3 Results and Discussion

To test the possibility of using SU-8 to fabricate carbon nano-wires, samples were pyrolyzed in an inert environment. Samples prepared by Method 1 failed the pyrolyzation as the deposited wires were mostly liquid before carbonization. The fibers produced by Method 2 had a yield rate of 81 %. The diameters after pyrolysis were analyzed and measured using SEM micrographs.

Cardenas [6] states that the geometry of the carbon nano-wires is also an important characteristic that affects the carbon structure conductivity, mechanical and thermal characteristics and crystallinity. The conducted experiments showed some techniques and materials that have been applied to fabricate carbon nano-wires, as well as the effects that fabrication parameters have on the final geometry of the carbon structures. The new technique of electro-mechano-spinning (EMS) involved new polymer solutions along with a systematic deposition process. Cardenas [6] found that the EMS proposed manufacturing technique yielded normally distributed diameters of 204 *nm* with low variability, which is significantly reduced the uncertainty in the fabrication of carbon nano-wires.

6 Theoretical Framework

6.1 Photoresists

The electronic industry requires a sustainable raw material supply for its development [30]. Photoresists are a type of raw material used in microelectronics, which is composed by four main elements: a polymer (resin), a photoactive compound, a solvent, and an additive [24]. The additive requires to be with low molecular weight as it is intended to act as a photosensitive material. Photoresists are used within the manufacturing process of printed circuit boards [29]. Photoresists are classified into two categories. The resist is defined as positive if the radiation exposed material is soluble in photoresist developer; otherwise, for negative photoresist the exposed material remains to stay in the photoresist surface as it crosslinks upon exposure [13, 25], see Figure 6.1. In the manufacturing process of a semiconductor, the radiation sources which are often used in a lithography process are ultraviolet (UV) and X-ray [17].

The polymeric material is available on the broad market either in liquid or solid state; *MicroChem Corp.* (Westborough, MA, USA) is the principal provider of SU-8 photoresist. SU-8 and similar photoresists are inexpensive with good adhesion on the semiconductor surface and high sensitivity [29]. Epoxy resins are copolymer-thermosetting plastics which are normally produced by a chemical reaction process that involves epichlorohydrin and bisphenol-A compound [28]. An epoxy-based polymer is typically used to produce patterns by lithography with the application of UV radiation. Lithography is a technique to transfer patterns from a mask and then transferred onto the substrate [13, 32]. SU-8 is a epoxy-based negative photoresist with the advantages of being inexpensive with good mechanical properties, good chemical resistance, and good electrical isolation [32]. SU-8 photoresists are used in the production processes of MEMS [33]. Photoresist-wise, the contrast and quality level of UV radiation lithography is affected by the wavelengths of

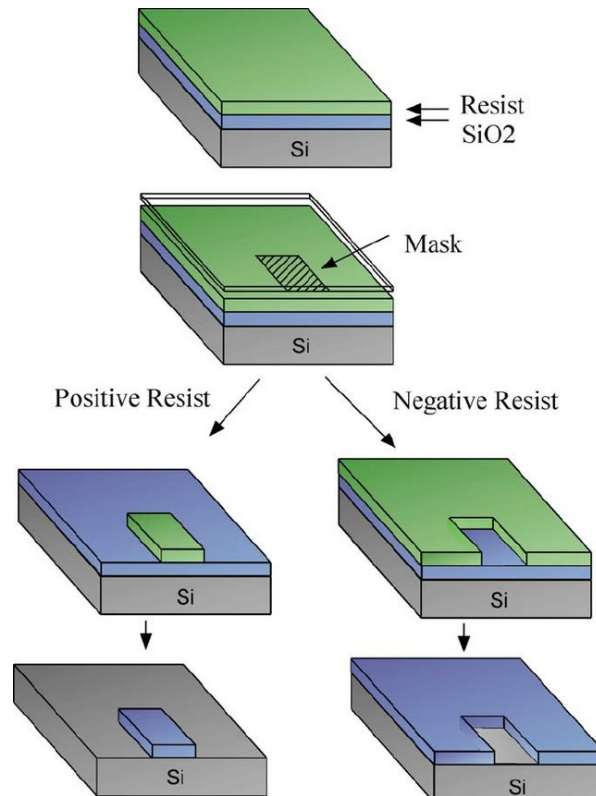


FIGURE 6.1: Positive and negative resist exposure and development [9]

radiation sources. The higher the sensitivity of the material, the better is the lithography process as it absorbs radiation energy with ease to perform photochemical reactions in forming patterns [33].

In summary, a photoresist is a "resin (polymeric) material which changes its dissolution rate in a liquid solvent, called a developer, under high energy radiation." [13]

6.2 Electro-Mechanical Spinning

Diverse polymer patterning techniques have been developed for the fabrication of nano-fibers, such as arc discharge [31], chemical vapor deposition, laser ablation [21], and vapor growth [18]. Nonetheless, those processes are expensive due to either the low product yield or the expensive equipment required. The electrospinning method (invented by Formhals Anton in 1934) can produce fibers with a range of diameters between 10 nm and 10 μ m [12, 2] from a polymer solution under the influence of an electrostatic force. The applied electric field and solution conductivity and viscosity is an important

parameter that affects the fiber diameter during the spinning along with other parameters such as jet length, solution viscosity surrounding gas, flow rate and the collector geometry [1, 14, 4, 26].

Even though electrospinning is an old invention [2], it is currently a trending topic among researchers [11, 22, 23]. One of the reasons electrospinning is to be studied is its potential to fabricate polymer nano-fibers from a variety of polymers. The technique allows the production of thin continuous fibers with ease, with diameters down to 3 nm in some cases, which is something difficult to achieve by other techniques. Furthermore, the basic set-up can be modified with ease to fabricate different fibers with diversified functionalities with different materials. The produced fibers can be aligned or unaligned. Besides, the electrospinning equipment is inexpensive and of small size, compared to the equipment of standard spinning techniques. On the other hand, the understanding of the electrospinning process has improved in the last years [15]. As Reneker and Yarin state: "Electrospinning has rapidly changed fiber making from a capital intensive, large scale process to a low cost, broadly applicable method that manufactures fibers on a laboratory bench, to serve diverse needs ranging from materials science and technology to life sciences and clinical medicine." [22]

The main components of the electrospinning technique are the fluid control unit (e.g. syringe pump) and a DC power supply. The process also requires a target electrode or combination of electrodes on which the fibers can be collected. Figure 6.2 describes a typical electrospinning set-up. [15]

Two sub-techniques can be derived from electrospinning depending on the distance between the dispensing electrode and the collector. The process in which the electrospun jet can be controlled near the tip is called NFES or near-field electrospinning. [7] Moreover, if the distance between the collector and the dispensing needle is greater, the configuration is known as FFES or far-field electrospinning. [19] The difference between NFES and mechano-electrospinning is the presence of a mechanical collector that allows higher precision when patterning. Figure 6.3 shows a typical near field mechano-electrospinning apparatus.

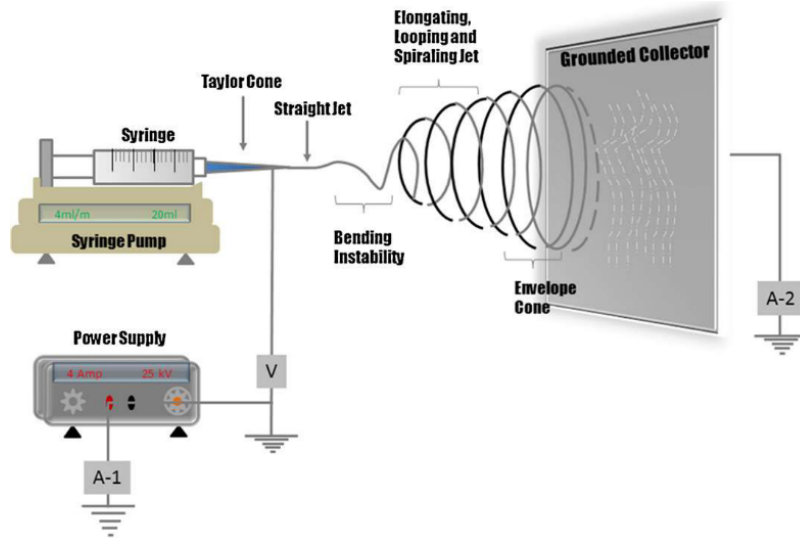
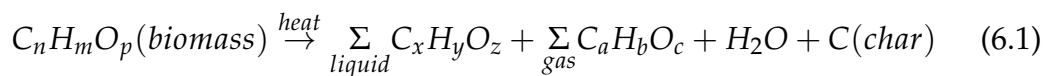


FIGURE 6.2: Typical far field electrospinning (FFES) set-up [15].

6.3 Pyrolysis

Pyrolysis is a technique that involves heating of biomass in the absence of air or oxygen at a maximum pyrolysis temperature. A small amount of oxygen can burn the structures and make them unusable [20]. Once the maximum pyrolysis temperature is reached, the temperature remains constant to produce solid char, liquids, and non-condensable products. In most cases the liquid product is the main interest of the pyrolysis process, and the properties of the pyrolysis products depend on the maximum pyrolysis temperature and the heating rate [20, 3].

The heating of large biomass molecules results in decomposition. The pyrolysis decomposition process comprises char, liquids (condensable gases) and non-condensable gases; where the condensable gases may suffer further decomposition into non-condensable gases such as CO , CO_2 , H_2 , and CH_4 . Equation 6.1 is a general representation of the pyrolysis decomposition reaction [3].



Pyrolysis yields solid products that are more energy dense than the initial biomass, however, the gas and liquid products are less energy dense [3]. The

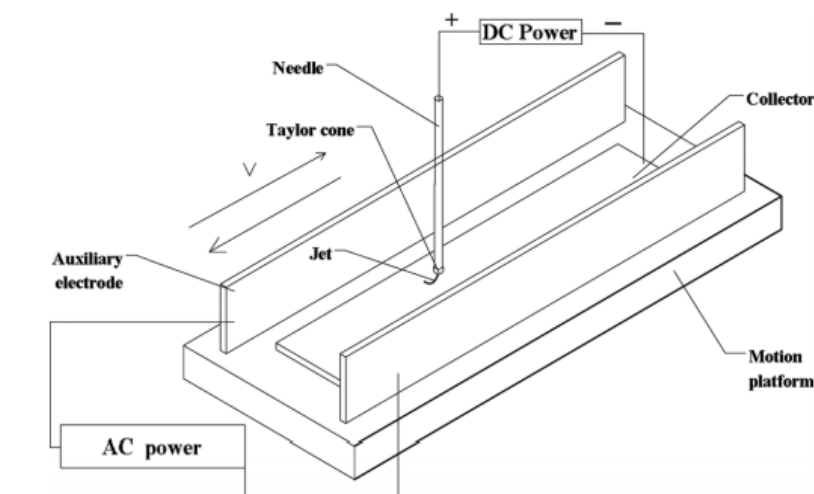


FIGURE 6.3: Typical near field electrospinning (NFES) set-up [34].

liquid product of pyrolysis is usually of colour black containing hydrocarbons with a large amount of oxygen and 20% water. When the liquid product is of interest, a rapid "quenching" (freeze) is required after pyrolysis to prevent further decomposition or reaction with other substances [3]. The solid yields of pyrolysis are usually around 85% carbon with some oxygen, hydrogen and other substances that are present within the initial biomass [3]. The biomass decomposition by pyrolysis produces non-condensable and condensable gases. The vapors (condensable gases) add up to the liquid yield of pyrolysis which is generated upon cooling. The gases (non-condensable gases) are comprised of ethylene, ethane, methane, carbon monoxide and carbon dioxide [3].

6.4 Carbon nano-wire

Carbon nano-wires (CMWs) are known as long, thin strings with diameters between 10 and 1 thousand *nm*; composed mostly by carbon atoms aligned parallel to the long axis of the fiber [19]. Carbon nano-wires are different from carbon nano-tubes, as CMWs are not composed by graphene sheets in cylindrical form [19]. Carbon nano-wires are typically fabricated by electrospinning and pyrolysis/carbonization as the main processes. During the fabrication process, the polymer molecules are to be crosslinked to prevent melting during the subsequent pyrolysis. The carbonization step removes non-carbonized components in form of condensable and incondensable gases [3] to then yield carbon structures of about 50% to 75% of the mass of the original polymeric structure [19].

6.5 Polymer Solutions

Polymer solutions display viscoelastic properties that provide unique properties due to their macromolecules. their chains are long and entangled. When a shear force is applied, the solution creates a large interaction between the molecules, hence the viscosity depends not only on temperature and shear, but also molecular weight distribution and concentration. The solvent also affects the viscosity [8, 11, 4].

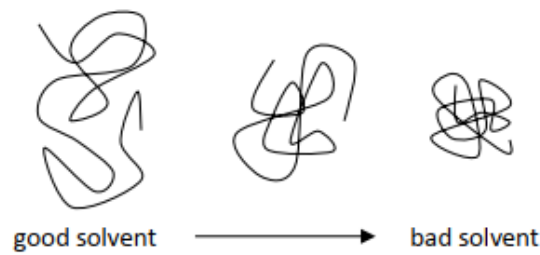


FIGURE 6.4: Effects in polymer chains dimensions due to solvent quality [8]

Figure 6.4 shows how the quality of a solvent affects the polymer distribution within the solution. Moreover the presence of electrolytes also modify the structure of the polymer threads. In non-ionic solvents, the charges are distributed along the chains and their own repulsion stretches the polymer threads into a more aligned configuration when an electrolyte is added, as detailed in Figure 6.5.

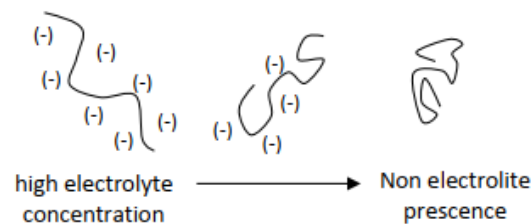


FIGURE 6.5: Effects of electrolyte in polymer chain dimensions [8]

6.6 Preliminary Experiments

6.6.1 Materials and Sample Preparation

To verify Flores' work [8], a series of rheological measurements have been executed. For that purpose, the solutions in Flores work were recreated as follows: The polymer system in the study is SU-8 2002 (SU-8, an epoxy-based negative photoresist) dissolved in cyclopentanone with poly(ethylene

oxide (PEO) to alter the viscoelastic properties of the polymer solution, and tetrabutylammonium tetrafluoroborate (TBATFB) to enhance the conductivity. Flores's results are listed in Section 5.1



FIGURE 6.6: Set 1 of the Recreation of Flores' Serie B'' Samples

The samples were prepared as follows, the suitable amounts of PEO and TBATFB were added to 5 mL of SU-8 in a 20 mL vial and stirred at 160 rpm during 1 hour at 75 °C. The proportions are represented in wt%. The samples with higher PEO concentration required to be stirred for more time to get rid of all PEO bundles. In order to avert cross-linking of SU-8 threads, during the stirring, the samples were isolated from light. a 5 mL syringe of was used to extract the solution from the vial. The recreated sample concentrations are depicted in Serie B within Table 5.1.

During the preliminary experiments, unlike to Flores' work, only the flow curve characterization was executed for two sample sets, as evidenced in Figures 6.6 and 6.7. The two sets were characterized by the generation of flow curves with a "TA Instruments" Discovery Hybrid Rheometer (DHR) at Tecnológico de Monterrey Campus Estado de México. The instrument's configuration was as follows:

- Geometry: 60 mm, cone plate, peltier plate steel
- Temperature: 20 °C



FIGURE 6.7: Set 2 of the Recreation of Flores' "Serie B" Samples

- Soak Time: 30.0 s
- Shear rate: 0.004 to 0.03 Hz
- Points per decade: 25

6.6.2 Results

As stated by Flores [8], it is expected an increase in viscosity with the increase of PEO concentration. However, the rheological results of set 1 (Figure 6.8) do not follow the expectations, as the 0.75 wt% PEO concentration is less viscous than the 0.50 concentration; and the 0.25 wt% PEO concentration is more viscous than the 0.75 concentration. On the other hand, results are not consistent with Flores' results as the viscosity values are as high as 200 Pa.s as depicted in Figure 6.8. The supposed values are to be around 0.0 and 10.0 Pa.s.

As shown in Figure 6.6, inconsistencies between Flores' work and the current flow curves have been for not stirring the samples until all the PEO lumps get completely dissolved in cyclopentanone. The lack of stirring, generated unknown PEO concentrations within each sample, hence the inconsistent results.

For set 2, the rheological flow curve characterization was performed in the

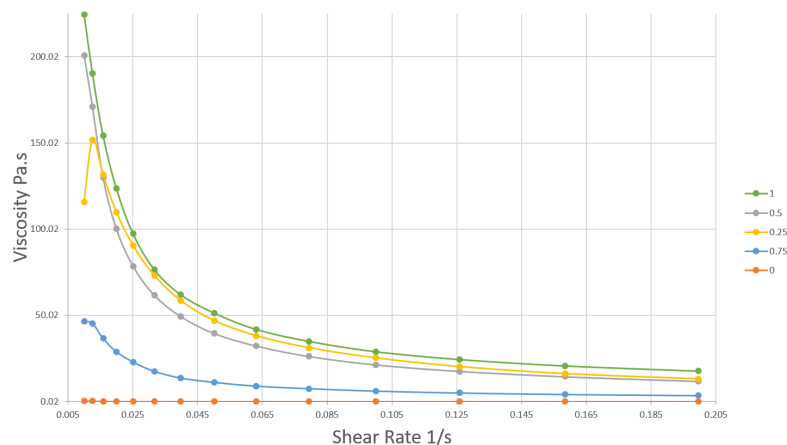


FIGURE 6.8: Set 1 Flow Curve Characterization of the Recreation of Flores' "Serie B" Samples

same way as in set 1, however, each sample was stirred for approximately 20 minutes before the characterization process. See Figure 6.7. Set 2 results, as depicted in Figure 6.9, are consistent with the expectations. However, unlike Flores' results, the replicated flow curves have a less stable/constant value as they present a more pronounced shear thinning behaviour. The difference in the shear thinning behaviours shown in Figure 6.9 (preliminary experiment, set 2 results) and Figure 5.8 (Flores' results [8]) may be caused by: 1) the use of different measurement instruments during the characterization process; and 2) the cyclopentanone solvent evaporation.

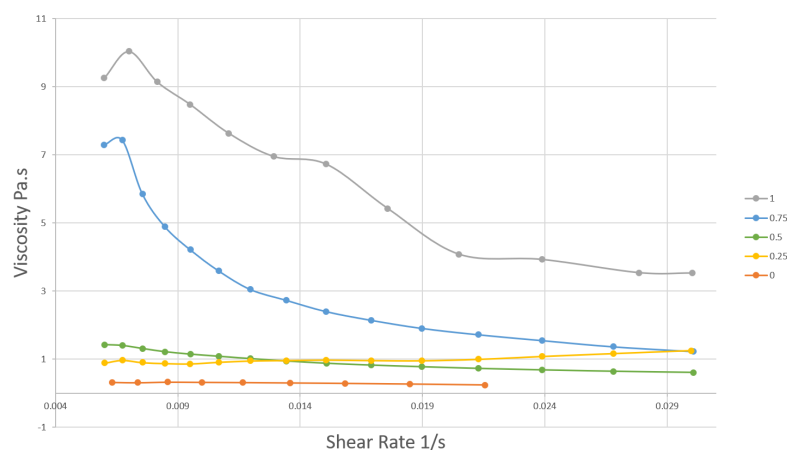


FIGURE 6.9: Set 2 Flow Curve Characterization of the Recreation of Flores' "Serie B" Samples

Table 6.1 compares the current zero shear viscosity measurements and Flores' measurements. The comparison shows that both measurements have

TABLE 6.1: Method 1 and Method 2 conditions and parameters [6]

Sample	PEO concentration [wt%]	Preliminary zero shear viscosity measurements [$Pa.s$]	Flores' zero shear viscosity measurements [$Pa.s$]
1	0.00	0.31	0.03
2	0.25	0.88	0.3
3	0.50	1.42	0.4
4	0.75	7.28	2
5	1.00	9.25	3

the same behaviour with similar proportions, as the zero shear viscosity increases with the increase of PEO concentration. However, the results show that the current measured values are approximately three times larger than Flores' measurements.

7 Methodology

The following describes the proposed work to be done to fulfill the objectives stated in this document. The tasks are grouped in several work packages as described below:

7.1 Preliminary Literature Review

The first step to the thesis development is the study of preliminary literature and related work. The purpose of this work package is the familiarization of the existing techniques such as: far and near field electrospinning, lithography, pyrolysis, carbonization and photopolymerization. On the other hand, some research is to be done in order to recognize if there are any efforts in the design of electrospun-able, photopolymerizable and pyrolysable polymer solutions.

Furthermore, the motive of this work package is to find common parameters that could link the techniques mentioned above for the fabrication of carbon nano-wires from polymer solutions that can be electrospun by NFES, photopolymerized and then pyrolyzed. This work package is to be carried out through the entire thesis development process, as the state-of-the-art may change within that period of time.

7.2 Evaluation of Fabrication Parameters

As the polymer solution is the principal input to the proposed technique (See Figure 1.1), it is required to identify and understand the fabrication parameters that have an impact on the quality of the carbon nano-wires. For that reason two tasks are to be executed:

- Study and identify the process parameters that influence the fabrication of carbon nano-wires

- Study and identify the rheological properties in polymer solutions that affect the electrospinning and pyrolysis techniques

7.3 Polymer Solution Design

Once the process parameters and rheological properties that affect the fabrication of carbon nano-wires are identified, the design process shall take place. This work package is to study polymer solutions that can be electrospun by NFES, photopolymerized and pyrolyzed. The polymer solution design will comprise of two steps:

- Prepare and test various polymer solutions with specific distinctions according to the identified solution properties and process parameters.
- Perform rheological analyses to determine if the prepared polymer solutions can be employed for the fabrication of carbon nano-wires.

7.4 Fabrication of Carbon Nano-wires

From the rheological analyses, determine and control the polymer solution properties and fabricate carbon nano-wires.

This work package intends to involve several manufacturing processes (near field electrospinning, photopolymerization, pyrolyzation and carbonization) for the fabrication of carbon nano-wires. This task will require the integration of several techniques:

- *Electrospinning* - to convert the polymer solution into polymer nano-fibers
- *Photopolymerization* - to change the chemical properties of the polymer solution and crosslink its molecules. This is to prevent the polymer to melt during pyrolysis [3].
- *Pyrolysis* - to transform the polymer nano-fibers into conductive carbon nano-wires.

See Figure 1.1.

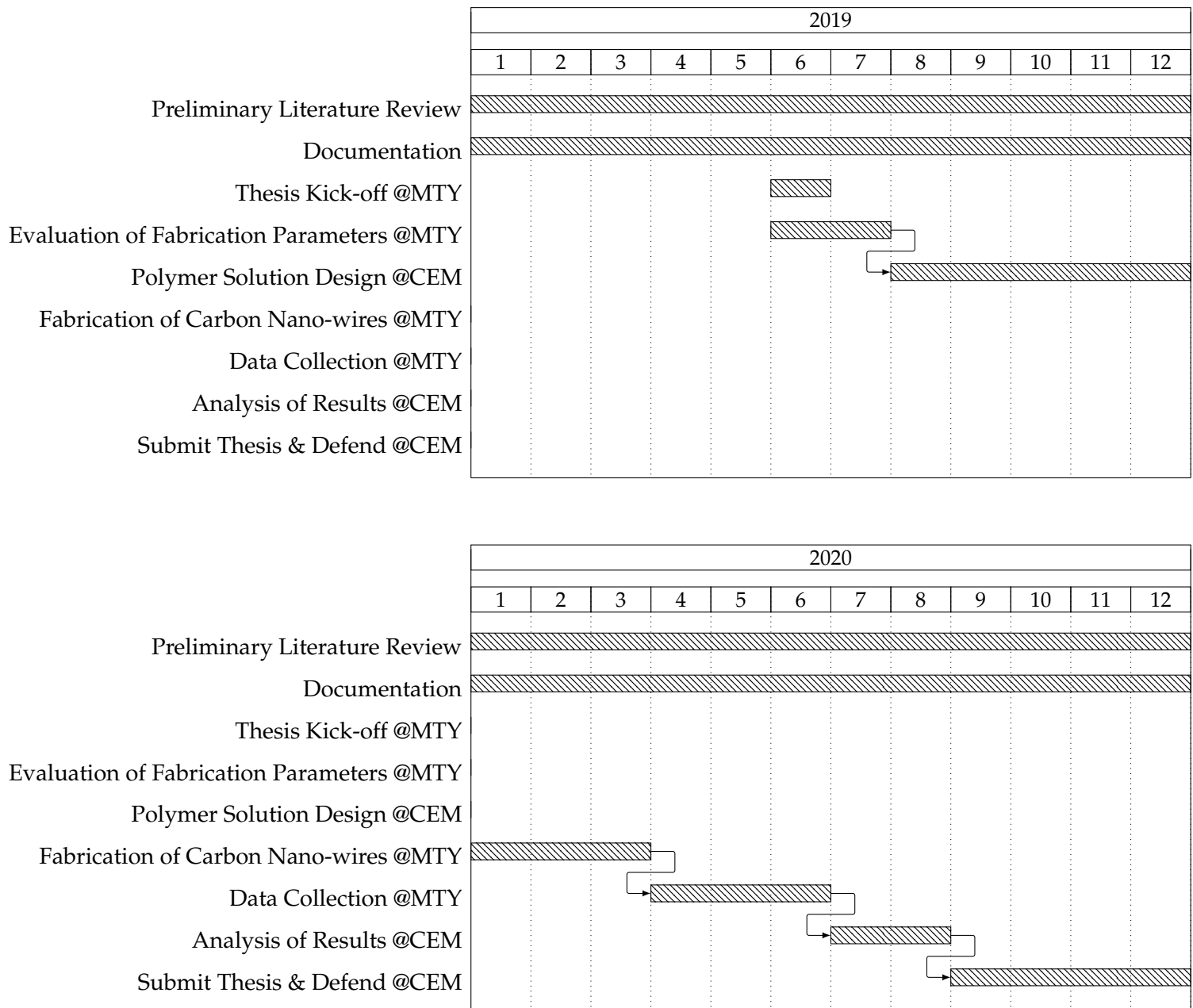
7.5 Data Collection and Analysis of Results

The data collection work package comprehends the study of the created carbon nano-wires using the new design polymer solution. The purpose is characterize the carbon nano-wires and compare them to the carbon nano-structures produced by existing techniques.

7.6 Documentation

Finally the documentation refers to the Thesis writing tasks. This task is intended to carry out through the entire thesis development process, as every work package above is to be referenced within the thesis document.

8 Work Plan



The previous are Gantt diagrams to show the work plan to be executed for the development of the proposed dissertation. The tasks mark with @CEM are to be carried out in Tecnológico de Monterrey campus Estado de México; consequently, the tasks mark with @MTY are to be performed in Tecnológico de Monterrey campus Monterrey.

References

- [1] Formhals Anton. "Method and apparatus for spinning". In: (Aug. 1938). DOI: <https://patents.google.com/?q=D01D5%2f0092>. URL: <https://patents.google.com/patent/US2349950A/en>.
- [2] Formhals Anton. *Process and apparatus for preparing artificial threads*. Dec. 1930. DOI: <https://patents.google.com/?q=D01D5%2f0076>. URL: <https://patents.google.com/patent/US1975504A/en>.
- [3] Prabir Basu. *Biomass Gasification, Pyrolysis and Torrefaction - Practical Design and Theory*. 3rd Editio. Elsevier, 2018. URL: <https://app.knovel.com/hotlink/pdf/id:kt011PGVNJ/biomass-gasification/biomass-ga-historical>.
- [4] Peter K Baumgarten. "Electrostatic spinning of acrylic microfibers". In: *Journal of Colloid and Interface Science* 36.1 (May 1971), pp. 71–79. DOI: [10.1016/0021-9797\(71\)90241-4](https://doi.org/10.1016/0021-9797(71)90241-4). URL: <https://www.sciencedirect.com/science/article/pii/0021979771902414>.
- [5] Jan Boer and Clemens Blitterswijk. *Tissue Engineering*. Ed. by Academic Press of Elsevier AP. 2nd. Safary O Reilly, 2014. URL: <https://learning.oreilly.com/library/view/tissue-engineering-2nd/9780124201453/XHTML/B9780124201453000109/B9780124201453000109.xhtml>.
- [6] Braulio Cárdenas. "Advanced Manufacturing Techniques for the Fabrication and Surface Modification of Carbon Nanowires". In: (2017), p. 160.
- [7] Albert Cisquella-Serra et al. "Study of the electrostatic jet initiation in near-field electrospinning". In: *Journal of Colloid and Interface Science* 543 (May 2019), pp. 106–113. ISSN: 0021-9797. DOI: [10.1016/J.JCIS.2019.02.041](https://doi.org/10.1016/J.JCIS.2019.02.041). URL: <https://0-www-sciencedirect-com.millennium.itesm.mx/science/article/pii/S0021979719302152>.
- [8] Domingo Ricardo Flores. "Role of rheological properties in near field electrospun fibers morphology". In: (2017), p. 130.
- [9] Hoggan et al. "Spin coating and photolithography using liquid and supercritical carbon dioxide". In: *Proceedings of SPIE-The International Society for Optical Engineering* 4690 (2002), pp. 1217–1223.
- [10] Kolin C Hribar et al. "Light-assisted direct-write of 3D functional biomaterials." In: *Lab on a chip* 14.2 (Jan. 2014), pp. 268–75. ISSN: 1473-0189. DOI: [10.1039/c3lc50634g](https://doi.org/10.1039/c3lc50634g). URL: <http://www.ncbi.nlm.nih.gov/pubmed/24257507>.

- [11] Zheng-Ming Huang et al. "A review on polymer nanofibers by electrospinning and their applications in nanocomposites". In: *Composites Science and Technology* 63.15 (Nov. 2003), pp. 2223–2253. ISSN: 0266-3538. DOI: 10.1016/S0266-3538(03)00178-7. URL: <https://www.sciencedirect.com/science/article/pii/S0266353803001787>.
- [12] Krishnan Jayaraman et al. "Recent Advances in Polymer Nanofibers". In: *Journal of Nanoscience and Nanotechnology* 4.1-2 (2003), pp. 52–65. URL: https://www.researchgate.net/publication/8591778%7B%5C_%7DRecent%7B%5C_%7DAdvances%7B%5C_%7Din%7B%5C_%7DPolymer%7B%5C_%7DNanofibers.
- [13] Stefan. Landis. *Nano-lithography*. ISTE, 2011, p. 325. ISBN: 9781848212114. URL: <https://learning.oreilly.com/library/view/nano-lithography/9781118621707/>.
- [14] L. Larrondo and R. St. John Manley. "Electrostatic fiber spinning from polymer melts. III. Electrostatic deformation of a pendant drop of polymer melt". In: *Journal of Polymer Science: Polymer Physics Edition* 19.6 (June 1981), pp. 933–940. DOI: 10.1002/pol.1981.180190603. URL: <http://doi.wiley.com/10.1002/pol.1981.180190603>.
- [15] Quan Li. *Chapter 7: Liquid Crystal-Functionalized Nano- and Microfibers Produced by Electrospinning - Liquid Crystals Beyond Displays: Chemistry, Physics, and Applications*. John Wiley & Sons, 2012. DOI: 9781118078617. URL: <https://learning.oreilly.com/library/view/liquid-crystals-beyond/9781118259535/chapter07.html>.
- [16] Marc J. Madou et al. "Controlled Continuous Patterning of Polymeric Nanofibers on Three-Dimensional Substrates Using Low-Voltage Near-Field Electrospinning". In: *Nano Letters* 11.4 (2011), pp. 1831–1837. ISSN: 1530-6984. DOI: 10.1021/nl2006164.
- [17] Harutaka Mekaru. "Performance of SU-8 Membrane Suitable for Deep X-Ray Grayscale Lithography". In: *Micromachines* 6.2 (Feb. 2015), pp. 252–265. DOI: 10.3390/mi6020252. URL: <http://www.mdpi.com/2072-666X/6/2/252>.
- [18] Arunan Nadarajah, Joseph G Lawrence, and Thomas W Hughes. "Development and Commercialization of Vapor Grown Carbon Nanofibers: A Review". In: *Trans Tech Publications* 380.1662-9795 (2008), pp. 193–206. DOI: 10.4028/www.scientific.net/KEM.380.193. URL: www.scientific.net/KEM.380.193.
- [19] S.K. Nataraj, K.S. Yang, and T.M. Aminabhavi. "Polyacrylonitrile-based nanofibers—A state-of-the-art review". In: *Progress in Polymer Science* 37.3 (Mar. 2012), pp. 487–513. ISSN: 0079-6700. DOI: 10.1016/J.PROGPOLYMSCI.2011.07.001. URL: <https://0-www-sciencedirect-com.millennium.itesm.mx/science/article/pii/S0079670011000931>.
- [20] Bidhan Pramanick et al. "Effect of pyrolysis process parameters on electrical, physical, chemical and electro-chemical properties of SU-8-derived carbon structures fabricated using the C-MEMS process". In: *Materials Today: Proceedings* 5.3 (Jan. 2018), pp. 9669–9682. ISSN: 2214-7853. DOI: 10.1016/J.MATPR.

- 2017.10.153. URL: <https://0-www-sciencedirect-com.millennium.itesm.mx/science/article/pii/S2214785317321788>.
- [21] Z F Ren et al. *Synthesis of Large Arrays of Well-Aligned Carbon Nanotubes on Glass*. Tech. rep. Science, 1998, pp. 1105–1107. DOI: [10.1126/science.282.5391.1105](https://doi.org/10.1126/science.282.5391.1105). URL: www.sciencemag.org.
- [22] Darrell H. Reneker and Alexander L. Yarin. “Electrospinning jets and polymer nanofibers”. In: *Polymer* 49.10 (May 2008), pp. 2387–2425. ISSN: 0032-3861. DOI: [10.1016/J.POLYMER.2008.02.002](https://doi.org/10.1016/J.POLYMER.2008.02.002). URL: <https://www.sciencedirect.com/science/article/pii/S0032386108001407>.
- [23] Jessica D. Schiffman and Caroline L. Schauer. “A Review: Electrospinning of Biopolymer Nanofibers and their Applications”. In: *Polymer Reviews* 48.2 (May 2008), pp. 317–352. ISSN: 1558-3724. DOI: [10.1080/15583720802022182](https://doi.org/10.1080/15583720802022182). URL: <http://www.tandfonline.com/doi/abs/10.1080/15583720802022182>.
- [24] Christine Schuster et al. “mr-NIL 6000LT – Epoxy-based curing resist for combined thermal and UV nanoimprint lithography below 50 °C”. In: *Microelectronic Engineering* 86.4-6 (Apr. 2009), pp. 722–725. DOI: [10.1016/J.MEE.2008.12.018](https://doi.org/10.1016/J.MEE.2008.12.018). URL: <https://www.sciencedirect.com/science/article/abs/pii/S0167931708006400>.
- [25] Maneesh Sharma et al. *Evaluation of microlithographic performance of ‘deep UV’ resists: Synthesis, and 2D NMR studies on alternating ‘high ortho’ novolak resins*. Tech. rep. 2. 2012, pp. 395–401. URL: www.ias.ac.in/chemsci.
- [26] Y.M. Shin et al. “Experimental characterization of electrospinning: the electrically forced jet and instabilities”. In: *Polymer* 42.25 (Dec. 2001), pp. 09955–09967. DOI: [10.1016/S0032-3861\(01\)00540-7](https://doi.org/10.1016/S0032-3861(01)00540-7). URL: <https://www.sciencedirect.com/science/article/pii/S0032386101005407>.
- [27] M.T.H Siddiqui et al. “Fabrication of advance magnetic carbon nano-materials and their potential applications: A review”. In: *Journal of Environmental Chemical Engineering* 7.1 (Feb. 2019), p. 102812. ISSN: 2213-3437. DOI: [10.1016/J.JECE.2018.102812](https://doi.org/10.1016/J.JECE.2018.102812). URL: <https://0-www-sciencedirect-com.millennium.itesm.mx/science/article/pii/S2213343718307358>.
- [28] Manoj Singla and Vikas Chawla. *Mechanical Properties of Epoxy Resin-Fly Ash Composite*. Tech. rep. 3. 2010, pp. 199–210. URL: http://file.scirp.org/pdf/JMMCE20100300003%7B%5C_%7D77044062.pdf.
- [29] Matthias Staab et al. “Applications of Novel High-Aspect-Ratio Ultrathick UV Photoresist for Microelectroplating”. In: *Journal of Microelectromechanical Systems* 20.4 (Aug. 2011), pp. 794–796. DOI: [10.1109/JMEMS.2011.2159098](https://doi.org/10.1109/JMEMS.2011.2159098). URL: <http://ieeexplore.ieee.org/document/5948317/>.
- [30] Sutikno Sutikno, Muhammad Hakim, and Sugianto Sugianto. “Synthesis of Phenolic-Based Resist Materials for Photolithography”. In: *Oriental Journal of Chemistry* 32.1 (Mar. 2016), pp. 165–170. DOI: [10.13005/ojc/320117](https://doi.org/10.13005/ojc/320117). URL: <http://www.orientjchem.org/vol32no1/synthesis-of-phenolic-based-resist-materials-for-photolithography/>.

- [31] Yu Wang et al. "Helical microtubes of graphitic carbon". In: *Acta Mechanica Sinica* 23.6 (2007), pp. 663–671. URL: https://www.researchgate.net/publication/260358247%7B%5C_%7DHelical%7B%5C_%7Dmicrotubes%7B%5C_%7Dof%7B%5C_%7Dgraphitic%7B%5C_%7Dcarbon.
- [32] Guang-Rui Xu, Miao-Jun Xu, and Bin Li. "Synthesis and characterization of a novel epoxy resin based on cyclotriphosphazene and its thermal degradation and flammability performance". In: *Polymer Degradation and Stability* 109 (Nov. 2014), pp. 240–248. ISSN: 0141-3910. DOI: 10.1016/J.POLYMDEGRADSTAB.2014.07.020. URL: <https://www.sciencedirect.com/science/article/pii/S0141391014002808>.
- [33] J Zhang et al. "Polymerization optimization of SU-8 photoresist and its applications in microfluidic systems and MEMS". In: *Journal of Micromechanics and Microengineering* 11.1 (Jan. 2001), pp. 20–26. DOI: 10.1088/0960-1317/11/1/304. URL: <http://stacks.iop.org/0960-1317/11/i=1/a=304?key=crossref.7e129e3392c38764a08aee10d49f57a6>.
- [34] Ziming Zhu et al. "Fabricated Wavy Micro/Nanofiber via Auxiliary Electrodes in Near-Field Electrospinning". In: *Materials and Manufacturing Processes* 31.6 (Apr. 2016), pp. 707–712. ISSN: 1042-6914. DOI: 10.1080/10426914.2015.1048464. URL: <http://www.tandfonline.com/doi/full/10.1080/10426914.2015.1048464>.